PRINT ISSN 1119-8362
Electronic ISSN 1119-8362

Full-text Available Online at
https://www.ajol.info/index.php/jasem
https://www.bioline.org.br/ja

J. Appl. Sci. Environ. Manage.
Vol. 26 (1) 91-104 January 2022

Linear and Non-linear Regression Analysis for the Sorption Kinetics of Rhodamine Dye from Aqueous Solution using Chitosan-Jackfruit nanocomposite

[1]JOHN BRITTO, S; [1]AMUTHA, E; [1]PUSHPALAKSMI, E; [1]JENSON SAMRAJ, J; [2]RAJADURAIPANDIAN, S; [2]GANDHIMATHI, S; *[1]ANNADURAI, G

[1]Division of Nanoscience, Sri Paramakalyani Centre for Excellence in Environmental Sciences, Manonmaniam Sundaranar University, Alwarkurichi - 627 412, India.
[2]Sri Paramakalyani College, Department of Chemistry, Alwarkurichi - 627412, India.
**Corresponding Author Email: gannadurai@msuniv.ac.in*

ABSTRACT: This paper presents experimental results such as the adsorbate-adsorbent chemical properties and chemical interaction as well as adsorption conditions. The experimental results were fitted to batch kinetic studies to obtain the characteristic parameters of each model. According to the evaluation using the Kinetic equation, the maximum sorption capacity at dye concentration was 19.6 (mg g^{-1}), pH 11.6 (mg g^{-1}) and temperature 24.2 (mg g^{-1}) Rhodamine dye were investigated. For all of the systems studied, the pseudo-first-order and pseudo-second-order model provided the best correlation of the kinetic experimental data. The results revealed that with increasing temperature and decreasing pH, ionic strength, and adsorbate concentration, dye removal efficiency has increased. Chitosan-Jackfruit nanocomposite could remove 90.2% dye from the solution containing 40 mg/L dye at 100 min. The results indicated that dye removal followed pseudo-second-order kinetic (R^2>0.99). According to the findings, Chitosan-Jackfruit nanocomposites an effective adsorbent for direct dye removal from wastewater.

DOI: https://dx.doi.org/10.4314/jasem.v26i1.15

Impact factor: **http://sjifactor.com/passport.php?id=21082**

Google Analytics: https://www.ajol.info/stats/bdf07303d34706088ffffbc8a92c9c1491b12470

Dates: Received: 23 August 2021; Revised: 21 December 2021; Accepted: 06 January 2022

Keywords: Adsorption, Rhodamine dye, Chitosan-Selenium Nanoparticle, Kinetic Studies

The current world is facing the problem of a shortage of pure drinking water because of limited sources of clean and pure water. Due to rapid growth in industries, a wide range of wastes is generated from the industries and is ultimately discharging into water resources, thereby affecting the quality and aesthetic of water Mahanta *et al.*, (2009); Ahmad and Kumar, 2010; Mittal *et al.*, (2010); Ansari *et al.*, (2011); Janaki *et al.*, (2012); Sajid *et al.*, (2016); Sajid *et al.*, (2018); Nidheesh *et al.*, (2018); Fang *et al.*, (2018); Siddiqui *et al.*, (2018); Nusrat Tara *et al.*, (2019). This is a very serious concern for developing countries. Among various wastes generated from the industries, color substances, particularly, dyes are the most dischargeable pollutants. Dyes are utilized in textile, paper printing, carpet, plastic, food, and cosmetic industries (Hussaini and Halbus, 2012); Subramanian *et al.*, (2018). Fabric and textile industries use dyes as a colorant on a large scale and commercially about 0.1 million dyes are available and approximately 7.0×10^5 ton dyes are produced annually Sen *et al.*, (2011); (Christie, 2017). The total dye consumption in textile industries is more than 10,000 tonnes per year, and about 10-15% of dyes are released into water from textile industries Dod *et al.*, (2012); Geetha *et al.*, (2015); (Akanksha and Sanjeev, 2018); Yao *et al.*, (2018); Yunhong *et al.*, (2018). Dyes can be mutagenic, carcinogenic, and allergenic to the human body, therefore, the contamination of dyes in water can be hazardous for aquatic organisms as well as humans Lin *et al.*, (2008); Ozdemir *et al.*, (2009); Gupta *et al.*, (2015). Dye wastewater that ends up in freshwater bodies causes havoc to aquatic species by increasing toxicity chemical oxygen demand (COD). It also affects the photosynthetic activities of aquatic plants through the reduction of light penetration Oliveira *et al.*, (2008). It has been reported that high COD, biological oxygen demand (BOD5) values, particulate matter (PM), and sediments, grease, and oil in effluents lead to the depletion of dissolved oxygen creating serious consequences on aquatic species Wang *et al.*, (2011). These activities generate highly colored effluents and should be treated before discharge in order to avoid negative environmental impacts. Unfortunately, most dyes are poorly biodegradable and cannot be effectively removed by conventional waste treatments Moran *et al.*, (1997); Sepulveda *et al.*, (2015). As tougher environmental legislation is enforced in most countries, there is a greater need for cost-effective treatment systems. In recent years, alternative wastewater treatment options for dye removal have been assessed including high-performance biological treatment (Sani and Banerjee, 1999), adsorption on activated carbon Allen *et al.*,

**Corresponding Author Email: gannadurai@msuniv.ac.in*

(1997), chemical coagulation, or physical retention by membranes Vandevivere *et al.,* (1998). However, most of these methods involve high operational costs in order to achieve the effectiveness required to meet strict environmental standards. On the other hand, the use of low-cost adsorbents offers an interesting option for the industrial implementation of adsorption-based removal of dyes. The adsorption process is one of the best water treatment techniques among various available methods. Adsorbent efficiently removes different pollutants and economical and eco-friendly. Among these, adsorption currently appears to offer the best potential for overall treatment, and it can be expected to be useful for a wide range of compounds. In this study, pomegranate peel activated carbon (PPAC) was evaluated as a new adsorbent for removal of a synthetic dye from an aqueous solution. We examined the effects of solution pH, Temperature, Dosages, and initial dye concentration on Rhodamine dye adsorption process onto Chitosan-Jackfruit nanocomposite from aqueous solution. Kinetic data were analyzed by different types of models were evaluated by pseudo-first-order; pseudo-second-order were also determined to understand the spontaneity of the adsorption process.

MATERIALS AND METHODS

Materials: All the necessary chemicals used in the study were of analytical grade. Rhodamine dye, Chitosan. Sodium tripolyphosphate was provided by Hi-media Private Ltd, Mumbai.

Preparation of Jackfruit sorbent: Jackfruit peel was obtained from a local fruit market in Alwarkurichi. The peels were first washed (more than 5 times) to remove any adhering dirt or moisture. They were then dried at room temperature (40°C) for 48 h, before being ball-milled from smaller particles of Jackfruit Sorbent Powder. The Jackfruit Peel powder was heated to 50°C in a water bath for about 2 days to remove color and pigments. The dried and ground Jackfruit peel powder (25g) was defatted by extraction with chloroform and methanol, and then placed at a ratio of 2:1, in soxhlet for 12 hrs to completely remove the color. The defatted Jackfruit peel was mixed with 350 ml of 0.2M Na_3PO_4 to bring the pH to 7.9 and to remove inactivates the pectic enzymes. After incubation overnight at 65 °C, the sample was filtered. The deproteinated Jackfruit peel powder was mixed with 100 ml of 0.50% ammonium oxalate (pH: 4.5). This mixture was shaken at 65°C in a water bath for 180 min then filtered. 10% of NaOH (25ml) was added to the depectinated Jackfruit peel powder. The mixture was shaken at 65°C in a water bath for 2 days, then filtered and washed in distilled water to remove the base. The hemicellulose-free Jackfruit peel powder was mixed with 100 ml of distilled water, 5 ml of 20% acetic acid, and 2.0g of NaCl. This mixture was shaken at 60°C in a water bath for 120 min and then filtered. The residue was washed with distilled water and ethanol to remove the acid and then dried at 50 °C in an oven for 16 hrs, finally producing smaller particles of Jackfruit Sorbent Powder.

Preparation of chitosan Nanoparticle: 3g of chitosan was weighed out and dissolved in 4% of the acidic acid solution followed by continuous stirring at room temperature for about 1 hour by using a magnetic stirrer and then 2g of sodium tripolyphosphate was dissolved in 200ml of distilled water and then added dropwise and freeze this solution (Chitosan Solutions) stand by 24 hrs and then precipitate was settled at the bottom and collected the precipitate and dried hot air oven 50^0C at 24 hrs. Finally prepared the chitosan nanoparticle was prepared.

Preparation of chitosan with Jackfruit Sorbent Powder: Chitosan-Jackfruit Nanocomposite was prepared in a 1:1 ratio. Firstly, 1g of chitosan nanoparticle and then 1g of Jackfruit sorbent powder was mixed within 100ml distilled water. And then this solution was shacked in shaken in 3 days. Next, the solution was filtered by using Whatman No. 1 filter paper. Finally, the particle was settled and then the particle was dried in Hot air oven for 24 hours, and then finally Chitosan-Jackfruit Nanocomposite was prepared.

Kinetic Studies: A 100 ml dye solution concentration (Rhodamine dye) 40 mg/L was treated with 1 g of the adsorbent material (Chitosan-Jackfruit nanocomposite) over some time with constant stirring. The following parameters were studied to elucidate the kinetics of adsorption.

(i) Effect of dosages: 1.0, 2.0 and 3.0g/L at constant temperature (30^0C), pH (6.8) and Rhodamine dye concentration 40 mg/L.

(ii) Effect of temperature: 30^0C, 45^0C and 60^0C at constant pH (6.8) Adsorbent dosages (Chitosan-Jackfruit nanocomposite) (1g/L) with 40mg/L Rhodamine dye concentration.

(iii) Effect of pH: 5.8, 6.8, and 9.4 at constant temperature (30^0C) and Adsorbent dosages (Chitosan-Jackfruit nanocomposite) (1g/L) with 40mg/L Rhodamine dye concentration.

The amount of dye adsorbed onto the adsorbent, q_e (mg/g), was calculated by a mass balance relationship: *Mass balance equation:* Throughout the experiment the mass balance equation was used, to find the amount of protein adsorbed in each flask which was determined by the equation (1),

$$Q = V(C_0 - C_t)/W \qquad (1)$$

Where Q - Adsorption capacity (mg/g), C_o - Initial concentration of Rhodamine dye (mg/L), C_t - Final concentration of Rhodamine dye (mg/L), V - Solution volume of Rhodamine dye (L), and W – Mass of adsorbent (g)

Hence, using this equation the amount of Rhodamine dye being adsorbed by the adsorbent was determined. All the experiments were conducted in duplicate and the results were presented as the average.

Adsorption Kinetics: The kinetics of adsorption was studied for its possible importance in the treatment of dye-containing industrial effluents (Cheremisinoff, 1995); Vandevivere *et al.*, (1998); Lin and Lin (1993). Numerous kinetic models have been proposed to elucidate the mechanism by which pollutants are adsorbed. To investigate the mechanism of the dye adsorption kinetic models were considered as follows. The kinetics of adsorption is important from the point of view that it controls the process efficiency Garg *et al.*, (2004); Mittal *et al.*, (2010). Various kinetic models have been used by various workers and different systems conform to different models but the Langergrens rate equations for the sorption of a solute from a liquid solution. To examine the controlling mechanism of adsorption processes such as mass transfer and chemical reaction; several kinetic models are used to test experimental data.

Table 1. Different Types of Pseudo Kinetic Equations

Type	Non-linear form	Linear form	Plot
Pseudo 1st order	$q = q_e(1 - exp^{-kt})$	$\log(q_e - q) = \log q_e - \frac{k_1 t}{2.303}$	$\log(q_e - q)\ vs\ t$
Type 1: Pseudo 2nd order	$q = \frac{k_2 q_e t}{1 + k_2 q_e t}$	$\frac{t}{q} = \frac{1}{k_2 q_e^2} + \frac{1}{q_e} t$	$\frac{t}{q}\ vs\ t$
Type 2: Pseudo 2nd order		$\frac{1}{q} = \frac{1}{k_2 q_e^2} + \frac{1}{t} q_e$	$\frac{1}{q}\ vs\ \frac{1}{t}$
Type 3: Pseudo 2nd order		$\frac{1}{t} = \frac{k_2 q_e^2}{q} - \frac{k_2 q_e^2}{q_e}$	$\frac{1}{t}\ vs\ \frac{1}{q}$
Type 4: Pseudo 2nd order		$\frac{q}{t} = k_2 q_e^2 - \frac{k_2 q_e^2 q}{q_e}$	$\frac{q}{t}\ vs\ q$
Type 5: Pseudo 2nd order		$\frac{1}{q_e - q_t} = \frac{1}{q_e} + k_2 t$	$\frac{1}{q_e - q_t}\ vs\ q$

Effect of Dosages: The initial concentration of the adsorbate in solution supplies an important driving force to overcome the mass transfer resistance between the solution and the solid adsorbent Almeida *et al.*, (2009). It has been demonstrated that enough contact time gives a chance to the interaction between the adsorbate and the adsorbent Hebeish *et al.*, (2011). To decide the impact of contact time on dye removal by Chitosan-Jackfruit nanocomposite at different dosages (1.0, 2.0, and 3.0 g/L) and the initial dye concentration of 40 mg/L, as per pertest, different time intervals (0 to 200 min) were investigated. The effect of adsorbent was the different weight of dosages on sorption of Rhodamine dye as shown in Figure. 1. It can be observed that as the dosages increases, the adsorption of dye increases. The result shows that there is a gradual increase in adsorption with increasing dosages.

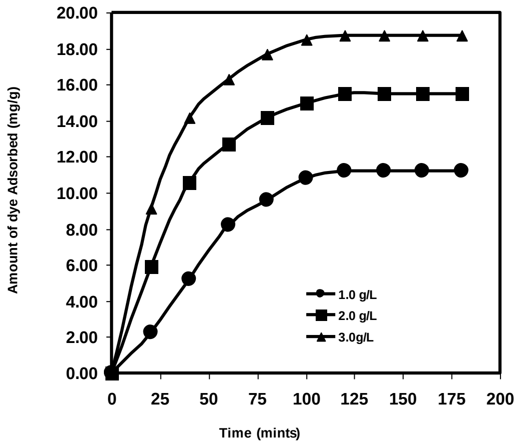

Fig 1. Effect of specific Rhodamine dye uptake at Different Dosages with time (min) (Chitosan-Jackfruit nanocomposite)

This figure shows that with increasing contact time, dye removal effectiveness increases, and the most elevated dye removal productivity and adsorption limit were gotten after 100 to 200 min for adsorbent dosages of 1.0, 2.0, and 3.0g/L, separately. As it is obvious from the outcomes, dye removal is fast in the underlying phases of sorption and afterward turns out to be moderate, and in the end contingent upon the adsorbent, portion accomplishes to balance at a particular time Hassan *et al.*, (2014); Amir Hossein Mahvi and Arash Dalvand (2020). By expanding the adsorbent portion from 1.0 to 3.0 g/L, the required time to reach equilibrium decreases. In the first stage of adsorption, many vacant sites are available and adsorption is fast Weber *et al.*, (2014), but later due to occupying and decreasing vacant sites, driving force decreases that lead to a decrease in the rate of adsorption. These results are in agreement with the results reported by Hebeish *et al.*, (2011); Amir Hossein Mahvi, and Arash Dalvand (2020).

The Effect of pH: The initial pH of the aqueous solution is an important parameter that influences the adsorption process Almeida *et al.*, (2009) by controlling the surface charge of the adsorbent, the adsorption availability of the dyes, and the degree of ionization of the atoms or molecules in the solution Errais *et al.*, (2011). The effect of pH on the adsorption process was studied at different pH values, namely, 5.8, 6.8, and 9.4 The results are represented in Figure. 2. This may be due to the number of positive charges on the sorbent surface which leads to the no rejection of the negatively charged dye molecule, and thereby increasing the adsorption Low and Lee (1997); Namasivayam *et al.*, (1996); Jumasiah *et al.*, (2005). In general, the uptakes are much higher in acidic solutions than those in neutral and alkaline conditions. The maximum values of the adsorption capacity ratio between acidic and alkaline conditions reach 5.5 to

6.8 Rhodamine dye on chitosan sorbent. The dye absorption may also derive support from the ion exchange reaction. According to Ho and McKay (1999) at lower pH more protons will be available to protonate amine groups of chitosan molecules to form groups $–NH_3^+$, thereby increasing electrostatic attractions between negatively charged dye anions and positively charged adsorption sites and causing an increase in dye adsorption. This explanation agrees with our data on the pH effect. It can be seen that the pH of aqueous solution plays an important role in the adsorption of Rhodamine dye onto Chitosan-Jackfruit Nanocomposite. All amino groups of the Chitosan-Jackfruit Nanocomposite are cationized and the dye anion pulled in strongly by electrostatic attraction Wang *et al.,* (2005); Nagarethinam and Mariappan, (2001). Higher dye removal efficiency at pH 6.8 can be attributed to the protonation of active groups on the surface of the adsorbent, which improves the electrostatic attraction of negatively charged dye molecules each dye molecule contains two anionic sulfonate groups toward positively charged adsorbent Mohanty *et al.,* (2006). With increasing pH, due to the deprotonation mechanism, the number of positively charged sites on the adsorbent decreases and as a result, the dye removal efficiency decreases Chiou and Li, (2002). Moreover, lower dye adsorption at higher pH is because of the presence of negatively charged hydroxyl ions which compete with the anionic dye molecules. For the adsorption sites Ho *et al.,* (2005).

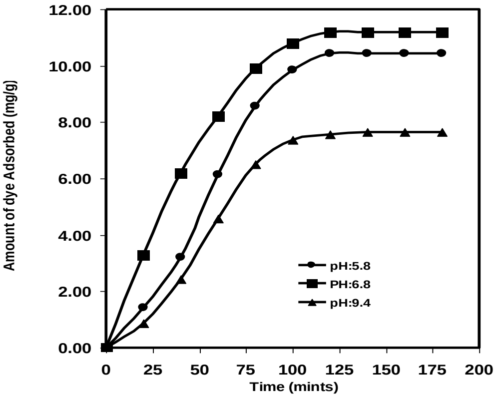

Fig 2. Effect of specific Rhodamine dye uptake at different pH with time (min) (Chitosan-Jackfruit nanocomposite)

Effect of Temperature: The adsorption decreases with an increase in temperature because the adsorption is an exothermic process. Figure. 3. Adsorption isotherms for the Rhodamine dye at 30^0C to 60^0 C, may also be explained on the basis that the solubility of the dyes is increased at higher temperature and adsorbate–adsorbent interactions decreased resulting in decreased adsorption.

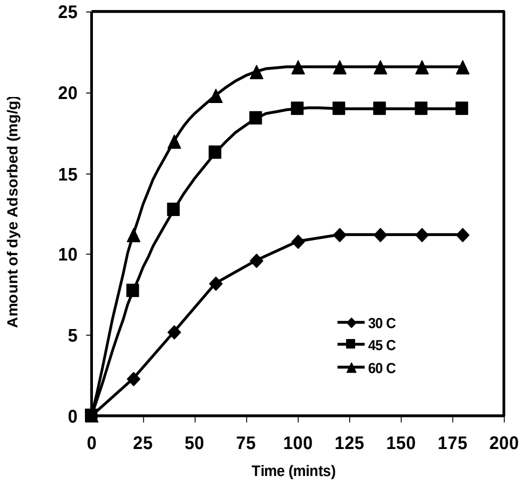

Fig 3. Effect of specific Rhodamine dye - uptake at different temperature with time (min) (Chitosan-Jackfruit nanocomposite)

This also indicated that desorption steps increase at a higher temperature than the adsorption. This type of adsorption is likely to be classified as reversible adsorption. A behavior similar to this has also been observed by Robinson *et al.,* (2002) on studies of adsorption of orange (IV) and orange G on biopolymer chitin. The adsorption of malachite green also decreases with the temperature in activated carbon (Aksu, 2001). The increase in temperature would increase the mobility of the large dye ion and also produces a swelling effect within the internal structure of the Chitosan-Jackfruit Nanocomposite Johann *et al.,* (2007); Batzias and Sidiras (2007). thus, enabling the large dye molecule to penetrate further. Therefore, the adsorption capacity should largely depend on the chemical interaction between the functional groups on the adsorbent surface and the adsorbate and should increase with a temperature rising Zeynep Eren and Filiz Nuran Acar (2007); Gopal *et al.,* (2014). The experimental rate curves of the Rhodamine dye on Chitosan-Jackfruit Nanocomposite at different Dosages, pH, and temperatures are shown in Figure. 1-3. In the beginning, the dyes molecules are adsorbed by the exterior surface of Chitosan-Jackfruit Nanocomposite. The adsorption rate is fast, and the adsorption of the exterior surface reaches saturation in a short time. At the same time, the dye enters into the Chitosan-Jackfruit Nanocomposite particle by the pore within the particle and is adsorbed by the interior surface of the particle. To have well known of the dye transient behavior onto Chitosan-Jackfruit Nanocomposite, the kinetic experimental results are analyzed by using the first-order kinetic model, second-order kinetic model, and various type of second-order kinetic model, respectively Hameed *et* *al.*, (2008). The models are given by the following equations. From a system design viewpoint, a lumped analysis of adsorption rates is thus sufficient for practical operation. A simple kinetic analysis of adsorption is the pseudo-first-order equation;

$$\frac{\mathrm{dq}_{\mathrm{t}}}{q_t} = K_1\left(q_{e_q} - q_t\right) \qquad (2)$$

After definite integration by applying the initial conditions q_t=0 at t=0 and q_t=q_t at t=t, equation (2) becomes;

$$\log\left(q_{e_q} - q_t\right) = \log q_{eq} - \frac{K_1}{2.303}t \qquad (3)$$

Where q_{eq} and q_t are amounts of dye adsorbed at equilibrium and at the time, in mg g-1 respectively, and the k_1 (mg g^{-1} min^{-1}) and q_e (mg g^{-1} min^{-1}), was applied to the present studies of dye adsorption. As such the values of log (q_e-q_t) vs t were calculated from the kinetic data of (Figure. 4 - 6) and plotted against time (Ho and McKay, 1998).

The first-order rate constant calculated from the plots is shown in (Table. 1).

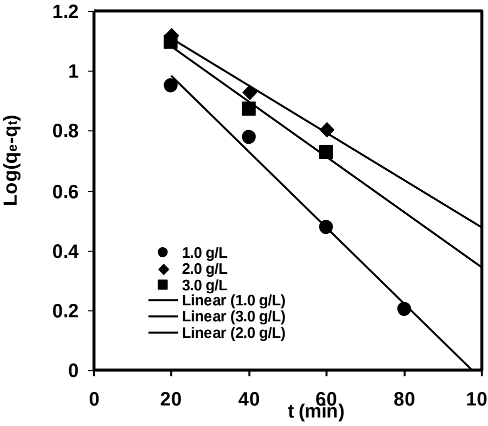

Fig 4. Pseudo-first order plot for the adsorption of Rhodamine dye using (Chitosan-Jackfruit nanocomposite) at various plots at Different Dosages

Figure. 4-6 shows the reversible first-order kinetic plot for the sorption of Rhodamine dye onto Chitosan- Selenium nanoparticle. The calculated K, K1, K2 values and their corresponding linear regression correlation coefficient R^2 1 values were shown in Table 2. The forward rate constant K_1 was much higher than the reverse rate constant K_2, confirming the domination of the adsorption process Jumasiah *et al.*, (2005); Konicki *et al.*, (2012). The linear regression correlation coefficient, R_2 1 values were found to fall in the range of 0.8607–0.9378 with an average value of 0.90136.

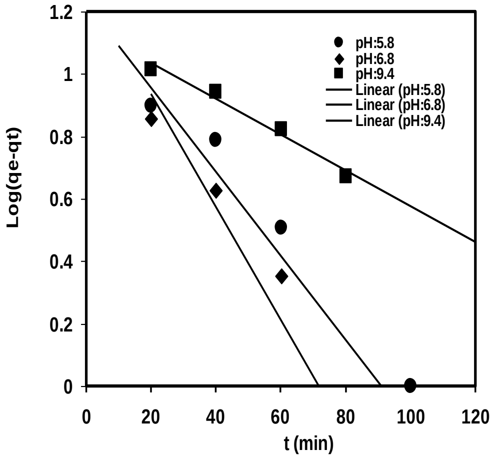

Fig 5. Pseudo-first order plot for the adsorption of Rhodamine dye using (Chitosan-Jackfruit Nanocomposite) at the various plot at pH

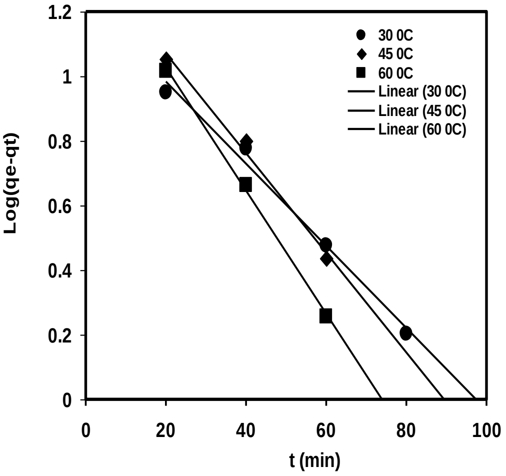

Fig 6. Pseudo-first order plot for the adsorption of Rhodamine dye using (Chitosan-Jackfruit Nanocomposite) at the various plot at Temperatures

This lower R^2 1 value confirms the applicability of this model but not an appropriate one. Adsorption kinetics for some systems can also be described by a pseudo-second-order reaction Franke *et al.*, (1987); Bolan, *et al.*, (1991). The pseudo-second-order equation based on adsorption equilibrium capacity may be expressed in the form;

$$\frac{\mathrm{dq}_{\mathrm{t}}}{q_t} = K_2\left(q_{eq} - q_t\right)^2 \qquad (4)$$

Where k_2 is the rate constant of pseudo-second-order adsorption. Integrating equation (4) and applying the initial conditions, we have

$$\frac{1}{(q_{eq} - q_t)} = \frac{1}{q_e} + K_2 t \qquad (5)$$

or equivalently,

$$\frac{t}{q_t} = \frac{1}{K_2 q_{eq}^2} + \frac{1}{q_e} t \qquad (6)$$

The equilibrium adsorption capacity (q_{eq}), and the second-order constants k_2 (g/mg min) can be determined experimentally from the slope and intercept of plot t/q_t versus t. The applicability of the pseudo-second-order models can be examined by the linear plot as shown in (Figure. 7-9). The correlation coefficient R^2 shows that the pseudo-second-order model an indication of chemisorption's mechanism that fits the experimental data slightly better than the pseudo-first-order model.

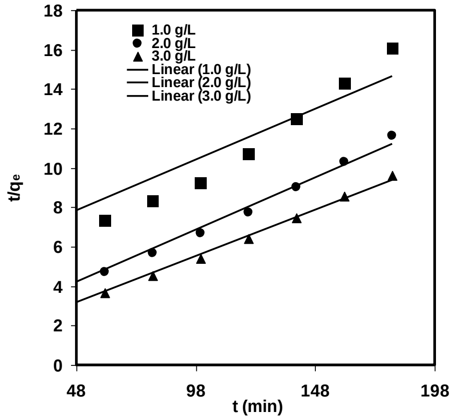

Fig 7. Pseudo-second order plot (Type - I) for the adsorption of Rhodamine dye using (Chitosan-Jackfruit nanocomposite) at different Dosages

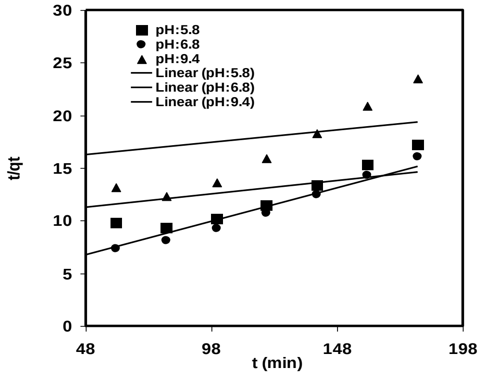

Fig 8. Pseudo-second order plot (Type - I) for the adsorption of Rhodamine dye using (Chitosan-Jackfruit nanocomposite) at various plots at Ph

Therefore, the adsorption of Rhodamine dye can be approximated more favorably by the pseudo-second-order model Ho and McKay (2000); Hasnain Isa *et al.,* (2007); Longhinotti *et al.,* (1998); Muhammad and Muhammad (2007). This model has been successfully applied to describe the kinetics of many adsorption systems. Calculated correlations are closer to unity for the second-order kinetics model; therefore, the adsorption kinetics could well be approximated more favorably by the second-order kinetic model for dye adsorption. The k_2 (mg g^{-1} min^{-1}) and q_e (mg g^{-1} min^{-1}) values as calculated are listed in (Table 2).

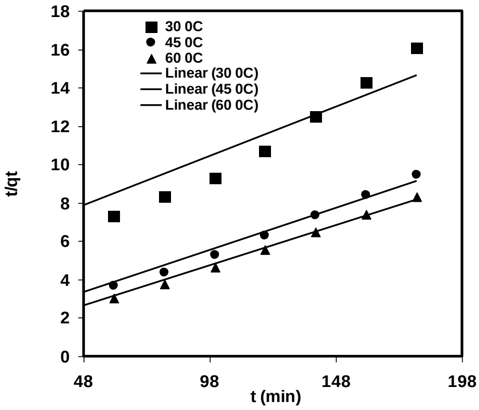

Figure 9. Pseudo-second order plot (Type - I) for the adsorption of Rhodamine dye using (Chitosan-Jackfruit nanocomposite) at the various plot at Temperatures

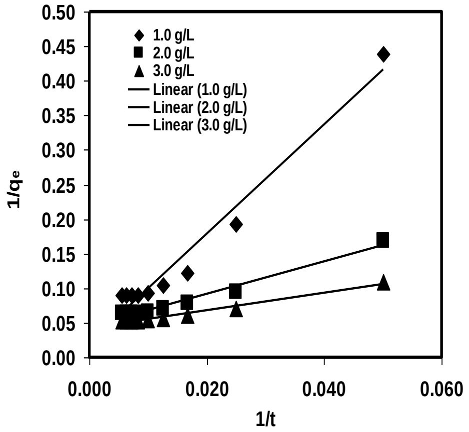

Fig 10. Pseudo-second order plot (Type-II) for the adsorption of Rhodamine dye using (Chitosan-Jackfruit Nanocomposite) at different Dosages

Fig. 7-9 shows the pseudo-second-order plot for Rhodamine dye onto Chitosan- Selenium nanoparticle. The pseudo-second-order rate constant K_2, the calculated qe value, and the corresponding linear regression correlation coefficient values R^2, K_2 is given in Table 3. At all different dosages, pH, and temperature, the linear regression correlation coefficient R^2, K_2 values were higher and ranged from 0.9646 to 0.9908. The higher R^2, K_2 values confirm that the sorption data are well represented by pseudo-second-order kinetics and supports the assumption behind the model that the sorption is due to chemisorption Robinson *et al.,* (2002); Sajid *et al.,* (2016); Schierz and Zanker (2009). The average R^2, K_2 value of 0.98354, which even better than that of R^2, K_1 values. This observation made clear that the sorption data tend to follow a pseudo-second-order kinetic model.

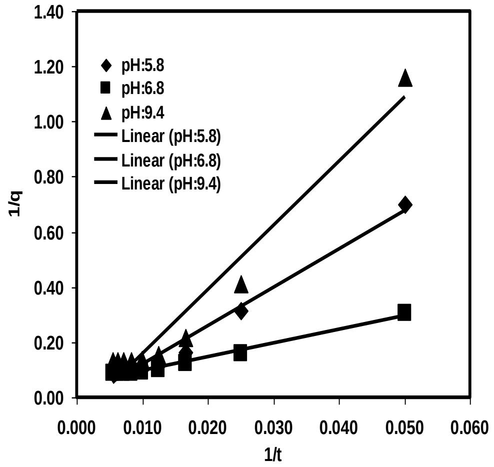

Fig 11. Pseudo-second order plot (Type-II) for the adsorption of Rhodamine dye using (Chitosan-Jackfruit Nanocomposite) at various plots at pH

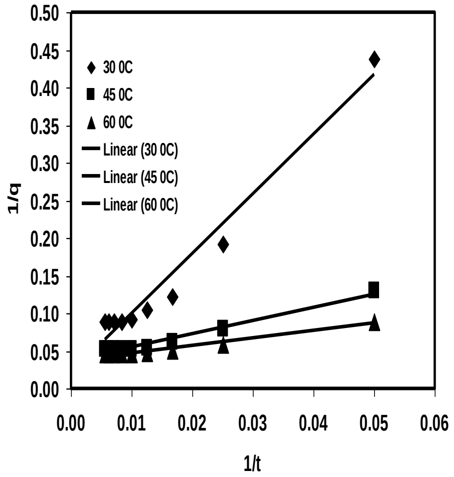

Fig 12. Pseudo-second order plot (Type-II) for the adsorption of Rhodamine dye using (Chitosan-Jackfruit Nanocomposite) at various plots at Temperatures

The initial sorption rate h was calculated using and the calculated values are shown in Table 3. From the Table, it was observed that the pseudo-second-order rate constant K_2 gets decreased with an increase in different dosages, pH, and temperature, and the initial sorption rate h was found to increase with the increase in different dosages and temperature Si *et al.,* (2015); Webber and Chakraborty (1974); Yan *et al.,* (2013). The relation for the predicted q_e, h calculated based on predicted q_e and second-order rate constant K_2 with different dosages and temperature were respectively. The relation between qe, h, and K_2 with a higher correlation coefficient confirms that all these parameters depend on the initial solute concentration

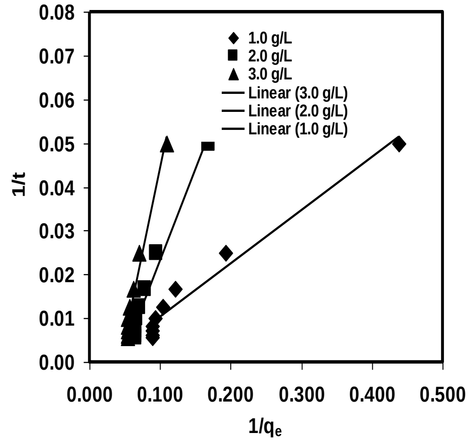

Fig 13. Pseudo-second order plot (Type-III) for the adsorption of Rhodamine dye using (Chitosan-Jackfruit Nanocomposite) at different Dosages

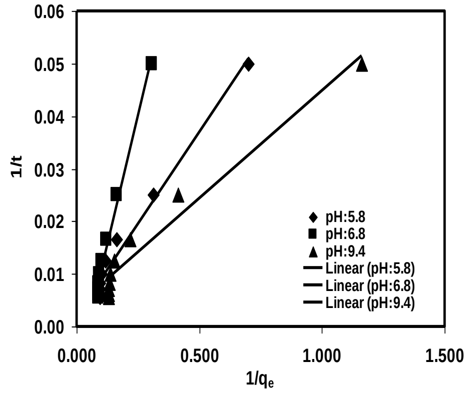

Fig 14. Pseudo-second order plot (Type-III) for the adsorption of Rhodamine dye using (Chitosan-Jackfruit Nanocomposite) at various plots at pH

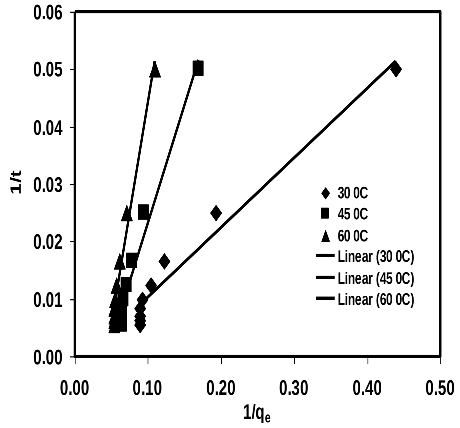

Fig 15. Pseudo-second order plot (Type-III) for the adsorption of Rhodamine dye using (Chitosan-Jackfruit Nanocomposite) at the various plots at Temperatures

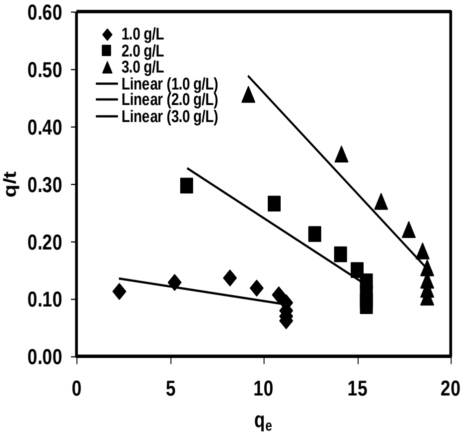

Fig 16. Pseudo-second order plot (Type-IV) for the adsorption of Rhodamine dye using (Chitosan-Jackfruit Nanocomposite) at different Dosages

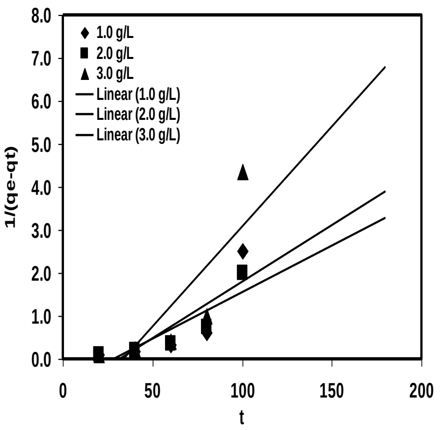

Fig 19. Pseudo-second order plot (Type-V) for the adsorption of Rhodamine dye using (Chitosan-Jackfruit nanocomposite) at different Dosages

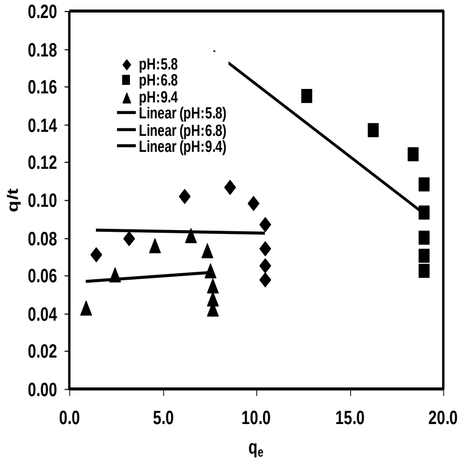

Fig 17. Pseudo-second order plot (Type-IV) for the adsorption of Rhodamine dye using (Chitosan-Jackfruit Nanocomposite) at various plots at pH

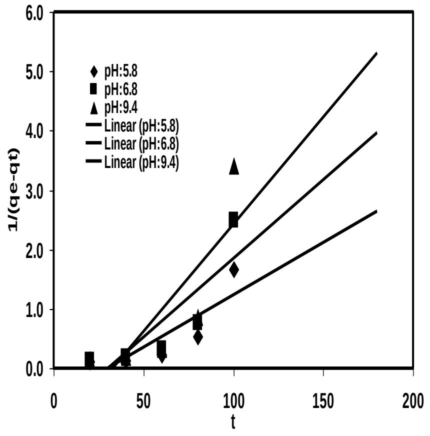

Fig 20. Pseudo-second order plot (Type-V) for the adsorption of Rhodamine dye using (Chitosan-Jackfruit nanocomposite) at various plots at pH

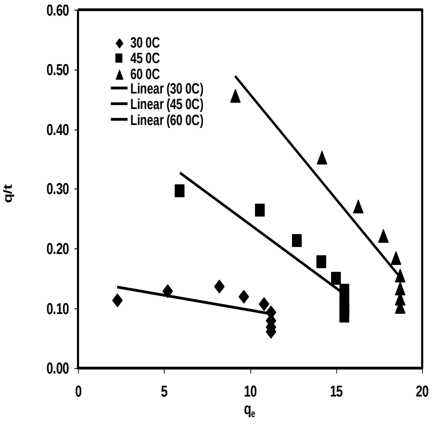

Fig 18. Pseudo-second order plot (Type-IV) for the adsorption of Rhodamine dye using (Chitosan-Jackfruit nanocomposite) at the various plot at Temperatures

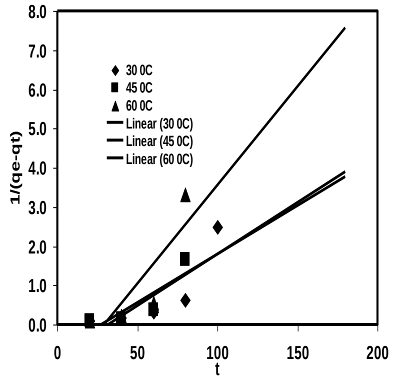

Fig 21. Pseudo-second order plot (Type-V) for the adsorption of Rhodamine dye using (Chitosan-Jackfruit nanocomposite) at the various plot at Temperatures

Table 2. Pseudo-first order rate constant at different dye concentration, pH, and temperature Rhodamine dye (Chitosan-Jackfruit nanocomposite)

Pseudo-first order		**Pseudo-first order rate constant**
Dosages (g/L)	1.0	K_1=0.02119; q_e=1.2677; R^2 = 0.9966
	2.0	K_1=0.0189; q_e=1.2679; R^2 = 0.99989
	3.0	K_1=0.02925; q_e=1.2374; R^2 = 0.9999
pH	5.8	K_1=0.0186; q_e=1.267; R^2 = 0.9353
	6.8	K_1=0.0114; q_e=1.269; R^2 = 0.9360
	9.4	K_1=0.0127; q_e=1.2374; R^2 = 0.9884
Temperature (^{0}C)	30	K_1=0.029; q_e=1.24; R^2 = 0.99989
	45	K_1=0.035; q_e=1.38; R^2 = 0.99989
	60	K_1=0.043; q_e=1.41; R^2 = 0.99989

Table 3. Pseudo second Order (Type - I) rate constant at different dye concentration, pH, and temperature Rhodamine dye (Chitosan-Jackfruit nanocomposite)

Pseudo second Order Type - I		**Pseudo second Order rate constant**
Dosages (g/L)	1.0	q_e = 19.46; K_2 = 0.00049; h = 0.18; R^2 = 0.8286
	2.0	q_e = 18.98; K_2 = 0.00162; h = 0.58; R^2 = 0.9871
	3.0	q_e = 21.28; K_2 = 0.00237; h = 1.07; R^2 = 0.9949
pH	5.8	q_e =39.06; K_2 =0.00007; h = 0.10; R^2 = 0.9270
	6.8	q_e = 15.70; K_2 = 0.00109; h = 0.27; R^2 = 0.9615
	9.4	q_e = 42.37; K_2 = 0.00004; h = 0.07; R^2 = 0.9140
Temperature (^{0}C)	30	q_e = 19.46; K_2 = 0.00049; h = 0.18; R^2 = 0.8286
	45	q_e = 22.78; K_2 = 0.00156; h = 0.81; R^2 = 0.9839
	60	q_e = 23.98; K_2 = 0.00270; h =1.55; R^2 = 0.9942

Table 4. Pseudo second (Type - II) rate constant at different dye concentration, pH, and temperature Rhodamine dye (Chitosan-Jackfruit nanocomposite)

Pseudo second Order Type – II		**Pseudo second Order rate constant**
Dosages (g/L)	1.0	q_e = 48.54; K_2 = 0.000054; h = 0.1261; R^2 =0.9666
	2.0	q_e = 22.32; K_2 = 0.000850; h = 0.4236; R^2 =0.9736
	3.0	q_e = 23.31; K_2 = 0.001445; h = 0.7850; R^2 =0.9776
pH	5.8	q_e = 45.66; K_2 = 0.000034; h = 0.0717; R^2 =0.9769
	6.8	q_e = 12.97; K_2 = 0.000255; h = 0.0428; R^2 =0.9579
	9.4	q_e =20.45; K_2 = 0.000484; h = 0.2024; R^2 =0.9827
Temperature (^{0}C)	30	q_e = 48.54; K_2 = 0.000054; h = 0.1261; R^2 =0.9666
	45	q_e = 26.81; K_2 = 0.000783; h = 0.5631; R^2 =0.7360
	60	q_e = 26.67; K_2 = 0.001437; h = 1.0216; R^2 = 0.9631

Table 5. Pseudo second (Type - III) rate constant at different dye concentration, pH, and temperature Rhodamine dye (Chitosan Jackfruit nanocomposite)

Linear regression of second-order kinetics-Rhodamine dye-Chitosan-Jackfruit nanocomposite: The Pseudo 2nd order equation may be written in four linearized types, the pseudo- 2nd order constants q_e and K_2 values can be calculated utilizing plotting among Type 1: t/q versus t, Type 2: 1/q as opposed 1/(q_e-q_t) vs t as opposed to t, Pseudo 2nd order isotherm, respectively as shown in Figure. 10 - 21.

Similarly, the pseudo-first-order isotherm constants K_1 can be calculated from the plot of log (q_e-q) as opposed to t, and the R^2 value is used to locate the first-rate becoming isotherm. The linear approach does no longer checks whether the experimental information is linear Low and Lee, (1997); Lin and Lin (1993). It assumes the experimental facts were linear and predicts the slope and intercept that makes an instant line that predicts the first-class-fit of experimental equilibrium statistics Ho and McKay (2000); Ho *et al.,* (2005); Hasnain Isa M *et al.,* (2007).

The linear method assumes that the scatter of points around the road follows a Gaussian distribution and the mistake distribution is equal at every price of X.

The linear technique simply predicts the Y for the corresponding X.

It considers best the mistake distribution along the Y-axis irrespective of the corresponding X-axis ensuing within the extraordinarily determined parameters. Pseudo-second-order model and there are good-fit straight lines for all of the experimental data at different dosages (1.0, 2.0, and 3.0g/L), pH (5.8, 6.8 and 9.4), and 20^{0}C. 45^{0}C and 60^{0}C.

It means that the pseudo-second-order equation (Type 4-7) can well predict the rate behavior of the Rhodamine dye onto Chitosan-Jackfruit Nanocomposite over the whole range, which strongly supports the validity of chemisorption probably involves in the adsorption of Rhodamine dye onto Chitosan-Jackfruit nanocomposite.

Conclusions: The removal of Rhodamine dye from aqueous solution using Chitosan-Jackfruit nanocomposite has been investigated under experimental conditions in batch mode. The adsorption of Rhodamine dye was found to be dependent on the adsorbent surface characteristics, adsorbent dosages and Temperature, pH, and initial dye concentration. Kinetics for the removal of Rhodamine dye were obtained and fitted to different kinetics model.

Table 6. Pseudo second Order (Type - IV) rate constant at different dye, concentration, pH, and temperature Rhodamine dye (Chitosan-Jackfruit nanocomposite)

Pseudo second Order Type – III		**Pseudo second Order rate constant**
Dosages (g/L)	1.0	$q_e = 1362.40$; $K_2 = 0.000170$; $h = 0.1468$; $R^2 =0.3725$
	2.0	$q_e = 104.22$; $K_2 = 0.000993$; $h = 0.4526$; $R^2 =0.8582$
	3.0	$q_e =35.05$; $K_2 = 0.001529$; $h = 0.8105$; $R^2 = 0.9160$
pH	5.8	$q_e = 1362.40$; $K_2 = 0.000170$;$h = 0.1468$; $R^2 = 0.3725$
	6.8	$q_e = 104.22 K_2 = 0.000993$; $h = 0.4526$; $R^2 =0.8582$
	9.4	$q_e = 35.05$; $K_2 =0.001529$; $h = 0.8105$; $R^2 = 0.9160$
Temperature (^{0}C)	30	$q_e = 29.36$; $K_2 = 0.000170$; $h = 0.1468$; $R^2 = 0.3725$
	45	$q_e = 21.55$; $K_2 = 0.000974$; $h = 0.4526$; $R^2 = 0.8582$
	60	$q_e = 23.03$; $K_2 = 0.001529$; $h = 0.8105$; $R^2 = 0.9160$

Table 7. Pseudo second Order (Type - V) rate constant at different dye concentration, pH, and temperature Rhodamine dye (Chitosan-Jackfruit nanocomposite)

Pseudo second Order Type - III		**Pseudo second Order rate constant**
Dosages (g/L)	1.0	$q_e = -1.22$; $K_2 = 0.0262$; $R^2 = 0.3725$
	2.0	$q_e = -1.62$; $K_2 = 0.0216$; $R^2 = 0.8582$
	3.0	$q_e = -0.64$; $K_2 = 0.0460$; $R^2 = 0.9160$
pH	5.8	$q_e = -1.94$; $K_2 = 0.0175$; $R^2 = 0.7189$
	6.8	$q_e = -1.24$; $K_2 = 0.0266$; $R^2 = 0.7208$
	9.4	$q_e = -0.85$; $K_2 = 0.0360$; $R^2 = 0.6771$
Temperature (^{0}C)	30	$q_e = -1.22$; $K_2 = 0.0262$; $R^2 = 0.6851$
	45	$q_e = -1.50$; $K_2 = 0.0216$; $R^2 = 0.7423$
	60	$q_e = -0.68$; $K_2 = 0.0460$; $R^2 = 0.7152$

REFERENCES

Ahmad, R; Kumar, R (2010). Conducting Polyaniline/iron oxide composite: A novel adsorbent for the removal of Amido black 10 B. *J. Chem. Eng. Data.* 55: 3489-3493.

Aksu, Z (2001). Biosorption of reactive dyes by dried activated sludge: equilibrium and kinetic modelling. *Biochem. Eng. J.* 7(1): 79–84.

Allen, SJ; Whitten, LJ; Murray, M; Duggan, O (1997). The adsorption of pollutants by peat, lignite and activated chars. *J. Chem. Technol. Biotechnol*. 68: 442-452.

Almeida, C; Debacher, N; Downs, A; Cottet, L; Mello, C (2009). Removal of methylene blue from colored effluents by adsorption on montmorillonite clay. *J. Colloid Interface Sci.* 332 (1): 46–53.

Ansari, R; Mosayebzadeh, Z (2011). Application of polyaniline as an efficient and novel adsorbent for azo dyes removal from textile wastewaters. *Chemical Papers*. 65(1): 1–8.

Batzias, FA; Sidiras, DK (2007). Simulation of dye adsorption by beech sawdust as affected by pH. *J. Hazard. Mater.* 141(3): 668–679.

Bolan, NS; Syers, JK; Sumner, ME (1991). Dissolution of various sources of gypsum in aqueous solutions and in soil. *J. Sci. Food Agric.* 57(4): 527–541.

Chiou, MS; Li, HY (2002). Equilibrium and kinetic modeling of adsorption of reactive dye on cross-linked chitosan beads. *J. Hazard. Mater.* 93(2): 233–248.

Christie, RM (2007). Environmental aspects of textile dyeing. Manchester: Textile Institute; Boca Raton.

Dod, R; Banerjee, G; Saini, S (2012). Adsorption of methylene blue using green pea peels (Pisum sativum): A cost-effective option for dye-based wastewater treatment. *Biotechnol. Bioprocess Eng.* 17(4): 862–874.

Eren, Z; Acar, FN (2007). Equilibrium and kinetic mechanism for Reactive Black 5 sorption onto high lime Soma fly ash. *Journal of Hazardous Materials*. 143(1–2): 226–232.

Errais, E; Duplay, J; Darragi, F; M'Rabet, I; Aubert, A; Huber, F; & Morvan, G (2011). Efficient anionic dye adsorption on natural untreated clay: Kinetic study and thermodynamic parameters. *Desalination.* 275 (1): 74–81.

Franke, MD; Ernst, WR; & Myerson, AS (1987). Kinetics of dissolution of alumina in acidic solution. *AIChE Journal.* 33(2): 267–273.

Garg, V K; Kumar, R; Gupta, R (2004). Removal of malachite green dye from aqueous solution by adsorption using agro-industry waste: a case study of Prosopis cineraria. *Dyes and Pigments.* 62(1): 1–10

Geetha, P; Latha, MS; Koshy, M (2015). Biosorption of malachite green dye from aqueous solution by calcium alginate nanoparticles: Equilibrium study. *J. Molecular Liquids.* 212: 723–730.

Gopal, N; Asaithambi, M; Sivakumar, P; Sivakumar, V (2014). Adsorption studies of a direct dye using polyaniline coated activated carbon prepared from Prosopis juliflora. *Journal of Water Process Engineering.* 2: 87–95.

Gupta, V K; Tyagi, I; Agarwal, S; Sadegh, H; Shahryari-ghoshekandi, R; Yari, M; Yousefi-nejat, O (2015). Experimental study of surfaces of hydrogel polymers HEMA, HEMA–EEMA–MA, and PVA as adsorbent for removal of azo dyes from liquid phase. *J. Molecular Liquids*. 206, 129–136.

Hameed, BH; Daud, FBM (2008). Adsorption studies of basic dye on activated carbon derived from agricultural waste: Hevea brasiliensis seed coat. *Chem. Eng. J.* 139(1): 48–55.

Hasnain Isa, M; Siew Lang, L; Asaari, FAH; Aziz, HA; Azam Ramli, N; Dhas, JPA (2007). Low cost removal of disperse dyes from aqueous solution using palm ash. *Dyes and Pigments*, 74(2), 446–453.

Hassan, AF; Abdel-Mohsen, AM; & Fouda, MMG (2014). Comparative study of calcium alginate, activated carbon, and their composite beads on methylene blue adsorption. *Carbohydrate Polymers*, 102: 192–198.

Hebeish, A; Ramadan, M. A; Abdel-Halim, E; & Abo-Okeil, A (2011). An effective adsorbent based on sawdust for removal of direct dye from aqueous solutions. *Clean Technologies and Environmental Policy.* 13(5): 713–718.

Ho, Y (2000). The kinetics of sorption of divalent metal ions onto sphagnum moss peat. *Water Research.* 34(3), 735–742.

Ho, Y. S; McKay, G (1998). A Comparison of Chemisorption Kinetic Models Applied to Pollutant Removal on Various Sorbents. *Process Safety and Environmental Protection*. 76(4): 332–340.

Ho, Y-S; Chiang, T-H; & Hsueh, Y-M (2005). Removal of basic dye from aqueous solution using tree fern as a biosorbent. *Process Biochemistry.* 40(1): 119–124.

Ho, YS; McKay, G (1999). Pseudo-second order model for sorption processes. *Process Biochemistry.* 34(5): 451–465.

Hussein, FH; Halbus, AF (2012, September 25). *Rapid Decolorization of Cobalamin*. International Journal of Photoenergy.

Iqbal, MJ; & Ashiq, MN (2007). Adsorption of dyes from aqueous solutions on activated charcoal. *Journal of Hazardous Materials.* 139(1): 57–66.

Janaki, V; Vijayaraghavan, K; Oh, B-T; Lee, K-J; Muthuchelian, K; Ramasamy, AK; Kamala-Kannan, S (2012). Starch/polyaniline nanocomposite for enhanced removal of reactive dyes from synthetic effluent. *Carbohydrate Polymers.* 90(4): 1437–1444.

Jumasiah, A; Chuah, TG; Gimbon, J; Choong, TSY; Azni, I (2005). Adsorption of basic dye onto palm kernel shell activated carbon: sorption equilibrium and kinetics studies. *Desalination.* 186(1–3), 57–64.

Kannan, N; Sundaram, MM (2001). Kinetics and mechanism of removal of methylene blue by adsorption on various carbons—a comparative study. *Dyes and Pigments.* 51(1): 25–40.

Konicki, W; Pełech, I; Mijowska, E; Jasińska, I (2012). Adsorption of anionic dye Direct Red 23 onto magnetic multi-walled carbon nanotubes-Fe3C nanocomposite: Kinetics, equilibrium and thermodynamics. *Chemical Engineering Journal.* 210: 87–95.

Li, F; Huang, J; Xia, Q; Lou, M; Yang, B; Tian, Q; Liu, Y (2018). Direct contact membrane distillation for the treatment of industrial dyeing wastewater and characteristic pollutants. *Separation and Purification Technology.* 195: 83–91.

Lin, JX; Zhan, SL; Fang, MH; Qian, XQ; & Yang, H (2008). Adsorption of basic dye from aqueous solution onto fly ash. *Journal of Environmental Management*. 87(1), 193–200.

Lin, SH; Lin, CM (1993). Treatment of textile waste effluents by ozonation and chemical coagulation. *Water Research*. 27(12): 1743–1748.

Longhinotti, E; Pozza, F; Furlan, L; Sanchez, M. de N. de M; Klug, M; Laranjeira, MCM; & Favere, VT (1998). Adsorption of Anionic Dyes on the Biopolymer Chitin. *Journal of the Brazilian Chemical Society*. 9(5), 435–440.

Low, KS; Lee, CK. (1997). Quaternized rice husk as sorbent for reactive dyes. *Bioresource Technology*. 61(2): 121–125.

Mahanta, D; Madras, G; Radhakrishnan, S; Patil, S (2009). Adsorption and Desorption Kinetics of Anionic Dyes on Doped Polyaniline. *The Journal of Physical Chemistry B*. 113(8): 2293–2299.

Mahvi, A. H; & Dalvand, A (2020). Kinetic and equilibrium studies on the adsorption of Direct Red 23 dye from aqueous solution using montmorillonite nanoclay. *Water Quality Research Journal.* 55(2): 132–144.

Mittal, A; Mittal, J; Malviya, A; Kaur, D; Gupta, VK (2010). Decolouration treatment of a hazardous triarylmethane dye, Light Green SF (Yellowish) by waste material adsorbents. *Journal of Colloid and Interface Science*. 342(2), 518–527.

Mohanty, K; Naidu, JT; Meikap, BC; Biswas, MN (2006). Removal of Crystal Violet from Wastewater by Activated Carbons Prepared from Rice Husk. *Industrial & Engineering Chemistry Research*. 45(14): 5165–5171.

Moran, C; Hall, ME; Howell, R (2008). Effects of sewage treatment on textile effluent. *Journal of the Society of Dyers and Colourists*. 113(10): 272–274.

Namasivayam, C; Muniasamy, N; Gayatri, K; Rani, M; Ranganathan, K (1996). Removal of dyes from aqueous solutions by cellulosic waste orange peel. *Bioresource Technology.* 57(1): 37–43.

Natarajan, S; Bajaj, HC; Tayade, RJ (2018). Recent advances based on the synergetic effect of adsorption for removal of dyes from waste water using photocatalytic process. *Journal of Environmental Sciences*. 65: 201–222.

Nautiyal, A; Shukla, SR (2018). Silver nanoparticles catalyzed reductive decolorization of spent dye bath containing acid dye and its reuse in dyeing. *Journal of Water Process Engineering.* 22: 276–285.

Nidheesh, PV; Zhou, M; & Oturan, MA (2018). An overview on the removal of synthetic dyes from water by electrochemical advanced oxidation processes. *Chemosphere*. 197: 210–227.

Oliveira, LS; Franca, AS; Alves, TM; Rocha, SDF (2008). Evaluation of untreated coffee husks as potential biosorbents for treatment of dye contaminated waters. *Journal of Hazardous Materials*. 155(3), 507–512.

Osma, JF; Saravia, V; Toca-Herrera, JL; Couto, SR. (2007). Sunflower seed shells: A novel and effective low-cost adsorbent for the removal of the diazo dye Reactive Black 5 from aqueous solutions. *Journal of Hazardous Materials.* 147(3): 900–905.

Ozdemir, O; Turan, M; Turan, AZ; Faki, A; Engin, AB (2009). Feasibility analysis of color removal from textile dyeing wastewater in a fixed-bed column system by surfactant-modified zeolite (SMZ). *Journal of Hazardous Materials*. 166(2), 647–654.

P, CN (2005). Handbook of Water and Wastewater Treatment Technologies. New Delhi Elsevier. Pp 576

Pi, Y; Li, X; Xia, Q; Wu, J; Li, Y; Xiao, J; Li, Z (2018). Adsorptive and photocatalytic removal of Persistent Organic Pollutants (POPs) in water by metal-organic frameworks (MOFs). *Chemical Engineering Journal.* 337: 351–371.

Robinson, T; Chandran, B; Nigam, P (2002). Removal of dyes from an artificial textile dye effluent by two agricultural waste residues, corncob and barley husk. *Environment International*. 28(1–2): 29–33.

Sajid, M; Basheer, C; Narasimhan, K; Buhmeida, A; Al Qahtani, M; Al-Ahwal, M (2016). Nature Environment and Pollution Technology An International Quarterly Scientific Journal Review Research Paper Persistent and Endocrine Disrupting Organic Pollutants: Advancements and Challenges in Analysis, Health Concerns and Clinical Correlates. *Nat. Environ. Pollut. Technol*, 15: 733–746.

Sajid, M; Nazal, MK; Ihsanullah, Baig, N; Osman, AM (2018). Removal of heavy metals and organic pollutants from water using dendritic polymers based adsorbents: A critical review. *Separation and Purification Technology*. 191: 400–423.

Sani, RK; Banerjee, UC (1999). Decolorization of triphenylmethane dyes and textile and dye-stuff effluent by Kurthia sp. *Enzyme and Microbial Technology*. 24(7): 433–437.

Schierz, A; Zänker, H (2009). Corrigendum to “Aqueous suspensions of carbon nanotubes: Surface oxidation, colloidal stability and uranium sorption” [Environmental Pollution 157 (2009) 1088–1094]. *Environmental Pollution.* 157(10): 2891.

Sen, TK; Afroze, S; Ang, HM (2010). Equilibrium, Kinetics and Mechanism of Removal of Methylene Blue from Aqueous Solution by Adsorption onto Pine Cone Biomass of Pinus radiata. *Water, Air, & Soil Pollution.* 218(1–4): 499–515.

Sepúlveda, L; Fernández, K; Contreras, E; & Palma, C (2004). Adsorption of Dyes using Peat: Equilibrium and Kinetic Studies. *Environmental Technology*. 25(9): 987–996

Si, J; Yuan, T-Q; Cui, B-K (2014). Exploring strategies for adsorption of azo dye Congo Red using free and immobilized biomasses of Trametes pubescens. *Annals of Microbiology*. 65(1): 411–421.

Siddiqui, SI; Rathi, G; Chaudhry, SA (2018). Acid washed black cumin seed powder preparation for adsorption of methylene blue dye from aqueous solution: Thermodynamic, kinetic and isotherm studies. *Journal of Molecular Liquids.* 264: 275–284

Tahir, SS; Rauf, N (2006). Removal of a cationic dye from aqueous solutions by adsorption onto bentonite clay. *Chemosphere*. 63(11): 1842–1848

Tara, N; Siddiqui, SI; Rathi, G; Chaudhry, SA; Asiri, I; AM (2020, January 31). *Nano-engineered Adsorbent for the Removal of Dyes from Water: A Review*. Current Analytical Chemistry.

Vandevivere, PC; Bianchi, R; Verstraete, W (1998). Review: Treatment and reuse of wastewater from the textile wet-processing industry: review of emerging technologies. *Journal of Chemical Technology & Biotechnology.* 72(4): 289–302.

Wang, S; Li, L; Wu, H; Zhu, ZH (2005). Unburned carbon as a low-cost adsorbent for treatment of methylene blue-containing wastewater. *Journal of Colloid and Interface Science*. 292(2): 336–343.

Wang, Z; Xue, M; Huang, K; Liu, Z (2011). Textile Dyeing Wastewater Treatment. *Advances in Treating Textile Effluent*.

Weber, CT; Collazzo, GC; Mazutti, MA; Foletto, EL; Dotto, GL (2014). Removal of hazardous pharmaceutical dyes by adsorption onto papaya seeds. *Water Science and Technology*. 70(1): 102–107

Weber, TW; Chakravorti, RK (1974). Pore and solid diffusion models for fixed-bed adsorbers. *AIChE Journal*. 20(2): 228–238.

Wu, Y; Luo, H; Wang, H; Wang, C; Zhang, J; Zhang, Z (2013). Adsorption of hexavalent chromium from aqueous solutions by graphene modified with cetyltrimethylammonium bromide. *Journal of Colloid and Interface Science*. 394: 183–191.

Wu, Yao, Chen, L; Long, X; Zhang, X; Pan, B; Qian, J (2018). Multi-functional magnetic water purifier for disinfection and removal of dyes and metal ions with superior reusability. *Journal of Hazardous Materials*. 347: 160–167.

.